



## The Influence of High-Strength Bolts Stiffening on Flange Connection Behaviour

Izabela MAJOR<sup>1)\*</sup>, Maciej MAJOR<sup>2)</sup>, Krzysztof KULIŃSKI<sup>1)</sup>

<sup>1)</sup> *Department of Technical Mechanics and Engineering Graphics  
Faculty of Civil Engineering  
Częstochowa University of Technology*

Akademicka 3, 42-200 Częstochowa, Poland  
e-mail: kkulinski@bud.pcz.pl

\*Corresponding Author e-mail: imajor@bud.pcz.pl

<sup>2)</sup> *Department of Steel Structures and Building Materials  
Faculty of Civil Engineering  
Częstochowa University of Technology*

Akademicka 3, 42-200 Częstochowa, Poland  
e-mail: mmajor@bud.pcz.pl

Flange connections can commonly be seen in advertising board structures, which are subjected to wind loading. Depending on the structure's geometry, additional torsion forces should be taken into account. In this paper the static behaviour of a flange connection with high-strength bolts under torsion load has been discussed. The numerical analysis concerns two cases: a flange connection subjected only to a high-strength bolts prestressing load and a flange connection subjected to both – bolts prestressing force and torsion moment. The stated boundary problem has been solved with the use of SolidWorks software. The obtained numerical results show good agreement with the analytical method.

**Key words:** flange connection; high-strength bolts; tightening torque; torsion analysis; structural analysis.

### 1. INTRODUCTION

The use of bolts has such a long history, dating back to the time before Christ. It is believed that the first wooden bolts were used in water lifting devices in ancient Greece around 240 BC. Some experts differ in opinion and argue whether bolts were not developed even earlier, in ancient Egypt, before the Archimedes invention. On the basis of experts' considerations, the first wooden bolts were used in land irrigation systems and to bilge water from ships [1]. In the XVth century bolts and screws were used by Gutenberg in his printing devices, whereas

at the turn of the XVIth century the first draft designs of screw-cutting machines were drawn.

The most intense development of thread bolts and screws have occurred over the last one hundred years. Both classic mathematical methods and experimental studies were carried out to determine the load bearing capacity of bolts. Mentioned tests concerned different materials, such as the shape of the bolt head, the shape of the thread, etc. Subsequently, world technological development led to boundary problem-solving with the Finite Element Method (FEM) approach.

The mechanical performance of 8.8 grade high-strength bolts under tension load was investigated by HU *et al.* [2]. Through the experimental study, two different failure modes were observed, i.e. necking of the boltshank threaded portion and thread stripping. Moreover, a numerical analysis has also been performed to observe the failure mechanism for different constitutive material laws and different tolerance classes in threads. Through both analyses, it was stated that thread stripping failure was the result of the coating process with different tolerance classes. The structural bolts' failure mechanism for partially and fully threaded construction bolts was also the subject of interest by GRIMSMO *et al.* [3]. On the basis of experimental tests and numerical studies on M16 8.8 grade construction bolts it was stated that bolt fracture takes place when the nut is considerably further in distance from the bolt head, whereas thread failure occurs when the distance between the nut and the beginning of the thread is relatively small. Moreover, through the simulations one could observe that regardless of the nut strength, the failure mechanism can be observed in the thread, whereas with an additional nut thread the mentioned failure mode could be suppressed. The finite element approach to determine the effects of additional axial forces and the bending moment resulting from damaged bolts on the static response of a flange connection in an actual telecommunication tower was discussed in [4].

The behaviour of construction bolts and bolted connections under fire and post-fire conditions was discussed in [5–7]. Cyclic heating and cooling conditions have an influence on the mechanical properties of the structural high tensile bolts that were studied by KODUR *et al.* [8].

Studies connected with various aspects of end-plate connections were the subject of interest of KRISHNAMURTHY [9] in the late 1970s. After many numerical and experimental tests, a mathematical model was proposed describing the actual end-plate work with introduced safety coefficients in order to provide economic end-plate connection designs. Through recent studies, it was stated that in some cases of end-plate connections, i.e. extended end-plate connection, geometry and material properties only have a small effect on connection behaviour [10]. The influence of high-strength construction bolts' tightening torque on stress distribution in a beam-to-beam end-plate connection was discussed in [11]. A reliability analysis of the structural joints in a steel lattice tower under

different wind velocities was presented by SZAFRAN *et al.* [12]. It is worth noting that GRZEJDA [13] in his work presented a general systemic approach to the FEM modelling and calculations of arbitrary multi-bolted systems. Recently, investigations of utilising smart materials, i.e. Shape Memory Alloys (SMA), have also been taken into considerations in newly designed connections [14–16].

## 2. PROBLEM FORMULATION

In this paper the static behaviour of a flange connection with high-strength bolts subjected to torsion is discussed. Two different analyses are performed: the first one concerns the influence of only an in-plane compressive preload applied to the bolts, and the second one concerns a combination of the torsion and bolts preload force on the behaviour of a static connection, respectively. Stresses near the bolt shank in the section between two adjacent flanges and in the whole flange connection has been taken into consideration. Moreover, a numerical model covering the actual work of an individual bolt with an applied preload force is examined. The stated boundary problem has been defined and solved in SolidWorks software with the use of the finite element method. FEM is the standard in many commercial software systems which are used for the stress analysis of elements [17–19].

### 2.1. Numerical model

As a geometric model, a section of a flange connection for two steel tubes has been adopted. The flange is composed of a circular steel plate with a diameter of  $\varnothing 545$  mm and a thickness of 20 mm welded concentrically to the host tube with a diameter of  $\varnothing 273$  mm, a thickness of 10 mm, and a length of 200 mm. The flange part located under the inner host tube has a circular internal cut with a diameter of  $\varnothing 253$  mm, which in consequence reduces overall connection mass. In order to increase the overall connection rigidity against deformations, special steel ribs have been provided. On the basis of PN-EN 1993-1-1 and literature [20–22] theory, in the end to end-plate and flange connections the influence of additional ribs stiffness is not considered in the designing process. Hence, on the basis of national standards, greater thickness of end plate/flange is obtained due to hidden safety factors than it would result from pure static connection behaviour. Moreover, that way of connection design has economical validation – production of a thicker plate is easier and faster than cutting a number of small elements and then welding them to the host connection. Regardless of that, designers do not resign from that additional stiffness provided by ribs, which may be especially important in steel structures loaded eccentrically, i.e. by horizontal icicles in mountains.



## 2.2. Loads

The first numerical model is composed of two cylindrical tubes assembled with a flange connection, where high-strength bolts are used and where two different types of loading were taken into consideration. The first load concerns the case of an in-plane compressive preload applied to the bolts. According to the manufacturer [23], the maximum preload which may be applied to an individual bolt is 225 552 N. For the second loading to the structure, two opposing torsion moments are applied with a value of 15 kN · m. Point “A” marked on the wall of the cylindrical steel tube in Fig. 1 denotes the location of the applied torsion moment in a clockwise direction in regard to the  $Z$ -axis of the presented Cartesian coordinate system with a small icon. Point “B” denotes a tube wall to which a counter-clockwise torsion moment is applied, respectively.

In this paper half of the bolt preload force is applied to each connector in the flange model in order to significantly increase the effect of torsion onto that structure’s deformation and on the bolt shank stresses. It should be noted that the higher the bolt preload force, the higher the friction force between the flange plates, and in consequence the smaller influence of opposing rotations. Moreover, by applying 100% of the compressive preload to the high-strength bolt, thread failure may be observed in some cases. This phenomenon is connected with additional bolt coats, i.e. zinc. The additional material on the nut screw starts to grate and fill the empty spaces between both the bolt and the nut threads providing an additional force counter to the prestressed bolts.

Both ultimate (ULS) and serviceability (SLS) limit the state of the proposed geometric connection when the assumed loads are validated via the IdeaStatica program proving that the connection may be safely treated as correctly designed.

In the second numerical model, where only a single high-strength bolt under compressive preload is analysed, deformations and stresses under a maximum prestressing force have been taken into consideration.

## 2.3. Numerical model assumptions and boundary conditions

Since the static response of a flange connection and a single high-strength bolt under different types of loading is discussed in this paper, the boundary conditions applied in each model should provide the static equilibrium. In the flange connection model (see Fig. 1) full structures is analysed. On the inner tubes’ cylindrical wall, radial displacements have been fixed, whereas on both external  $XY$  surfaces of the cylindrical tubes in Fig. 1, the  $Z$ -axis displacements have been fixed, respectively.

The second numerical analysis covers the whole single high-strength bolt model. The bolt length has been determined along the  $X$  axis. Displacements in the  $Y$  and  $Z$  axis direction have been fixed at the point of crossing between the

$YZ$  plane located at the end of the bolt threaded shank and longitudinal axis. The  $X$ -axis displacements have been fixed on 20 mm of bolt thread measuring from the connection between the bolt shank and the beginning of the thread.

It is worth noting that in the static numerical analysis the influence of fillet welds connecting cylindrical tubes to flange plates and ribs to the tubes has been neglected. Moreover, the bolt heads and nuts were represented by cylindrical bodies with appropriate length and diameter dimensions. Contact without penetration between the flange plates and the bolts with flange plates have been adopted. Preload compressive force has been applied to the head bolt surfaces and to the inner surface of the nuts, respectively.

Both the single high-strength bolt and the flange connection numerical model have been discretized with 4-node tetrahedron finite elements. Meshing depending on curvature has been used, where the minimum and maximum size of the finite elements are assumed to be in the range from 1.0 up to 5 mm. In the flange connection, first the in-plane preload force influence on static behaviour was examined. Furtherly, a combination of the initial prestressed bolts and torsion moments were taken into consideration. The following material properties have been adopted: for the Young Modulus bolts  $E = 210$  GPa and Poisson's ratio is  $\nu = 0.28$ , whereas for other elements  $E = 210$  GPa and  $\nu = 0.30$ . The maximum tensile strength for flange plates, ribs and tubes is assumed to be 235 MPa, whereas for bolts 1000 MPa, respectively. Both analyses were performed with the use of SolidWorks software.

### 3. RESULTS AND DISCUSSION

In this section the numerical results covering stress distribution and deformations in a flange connection and single high-strength bolt are discussed. Due to two different realized tasks, this section has been divided into two subsections, where first the flange connection static behaviour with high tensile bolts under torsion moment is discussed, then the static behaviour of a single high-strength bolt, respectively.

#### 3.1. Flange connection

Von Mises stress distribution in the section of the flange connection where only an in-plane preload has been applied is presented in Fig. 2, whereas a combination of torsion moment with prestressed bolts is presented in Fig. 3.

As presented in Fig. 2 one may notice that with an introduction to the system of an initial bolt preload, only a small area near the bolt is affected by compression. This force provides higher friction forces between the flange plates, which in consequence may counteract the forces responsible for the connection

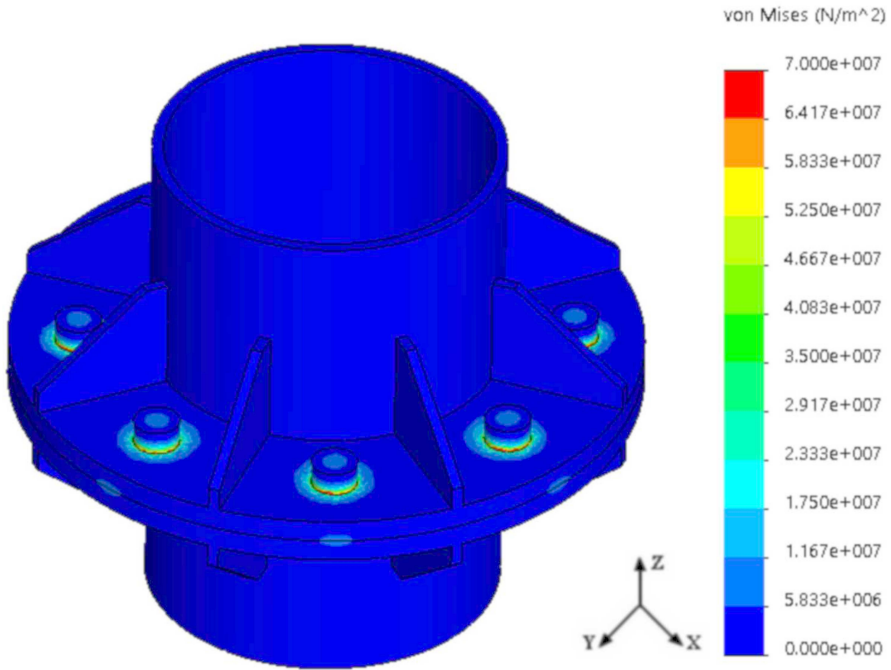


FIG. 2. von Mises stress in the flange connection where an in-plane compressive preload is applied to the high-strength bolts.

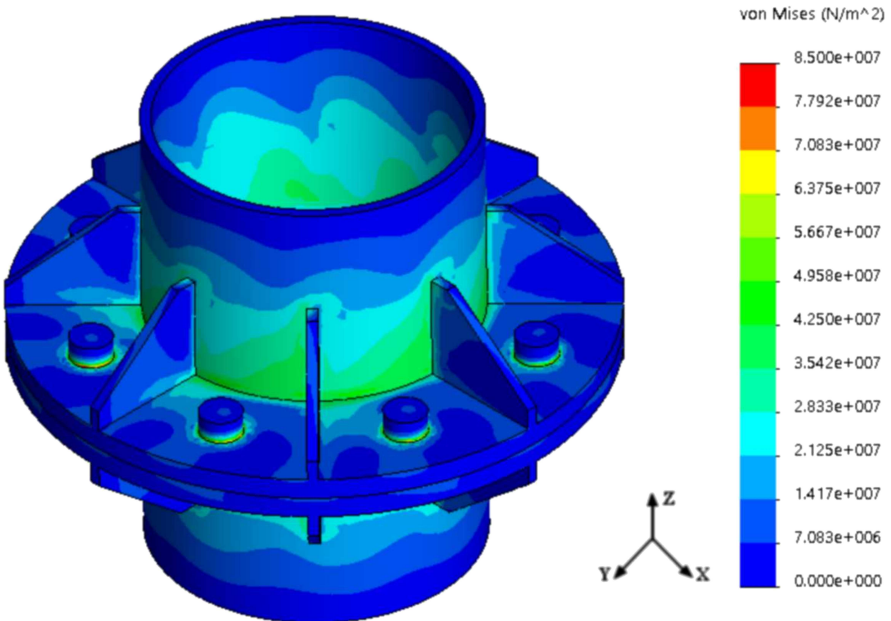


FIG. 3. von Mises stress in the flange connection from a combination of torsion moments and prestressed bolts.

rotation. In this paper, one of the main aims is to show how the structure deforms under applied torsion moments, thus friction forces have been neglected in the analysis. Moreover, the thickness of the flange plate in the nearest area of the bolts also changes. By applying prestress force to the bolts, the material between the bolt heads and nuts is very slightly compressed. According to this, the bolt washer needs a slightly greater force to be moved from that depression.

In Fig. 3 a small asymmetry in stress distribution has been observed, which is especially visible at the flange plates between ribs and on the inner tubes' walls. The asymmetry is connected with the two opposing acting torsion moments, which causes non-uniform deformation in the analysed structure. The maximum obtained stress in the connection is around 138.4 MPa, which is around 58.9% of allowed tensile stress for the S235 grade steel, whereas for the high-strength bolt 133.4 MPa is obtained, which is around 13.3% of bolt material tensile strength. In the bolt, the maximum stress value is observed at the connection of the shank and bolt head, which under the flange rotation leans on the flange plate hole's edge.

A verification of the numerical model has been performed via an analytical method in regard to the Hencky-Mises stress obtained in the bolt shank at the line of connection of flange plates resulting from a combination of prestressing and torsion moments. Normal stresses  $\sigma$  in the bolt shank at that line have been determined as  $\sigma = 81.40$  MPa and shear stress  $\tau = 13.00$  MPa. MHS  $\sigma_{\text{red}} = 84.46$  MPa. In the numerical model a cutting plane located at the line of connection between the flanges was introduced. Stress distribution in the bolt at this cutting plane location is presented in Fig. 4.

One may notice that the average stress in the numerical model for the bolt shank is equal to 85.16 MPa, thus the relative error is far beyond one percent and is equal to 0.83%.

Resultant displacements of the flange connection and its scaled deformation under a combination of torsion moments and the prestressing force of the bolts is presented in Fig. 5.

As presented in Fig. 5 a nearly symmetrical resultant displacement has been obtained, and the deformation of the discussed connection proves that the numerical model has been properly defined. It should be noted that the maximum read-out  $Z$ -axis displacement in point A in Fig. 5 is  $-0.019$  mm, whereas in point B  $0.008$  mm, respectively, where minus denotes the displacement in the opposite direction in regard to the coordinate system. The differences in  $Z$ -axis displacement result from the additional stiffness from rib near the point B. Without ribs, these displacements would be equal to  $-0.29$  and  $0.29$  for the same combination of loading, if only point B would be relocated at the intersection of external flange edge with one of the ribs' axis. In the same flange connection, loaded with greater values of torsion moment, the difference between the displacements would be significantly greater.

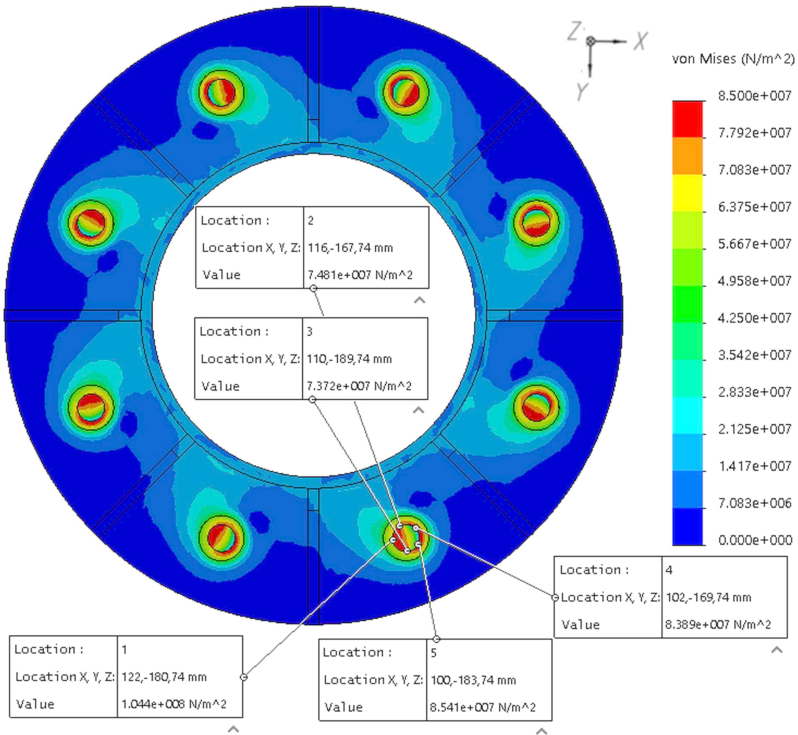


FIG. 4. von Mises stress distribution at the XY cutting plane located at the connection of the flange plates. MHS in different points at one of the bolt's shank.

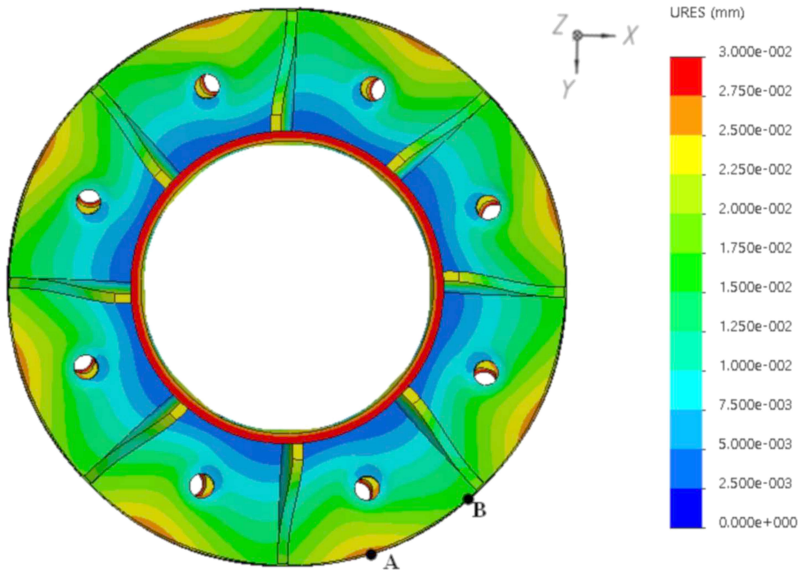


FIG. 5. Resultant displacements and scaled deformations in the cylindrical tubes flange connection.

### 3.2. Single high-tensile bolt under prestressing

In order to have a more complete analysis, deformations and MHS distribution of the authentically mapped single high-strength bolt numerical model subjected to the preload should have been discussed. Owing to that the von Mises stress plot and scaled deformations under the preload force are presented in Fig. 6.

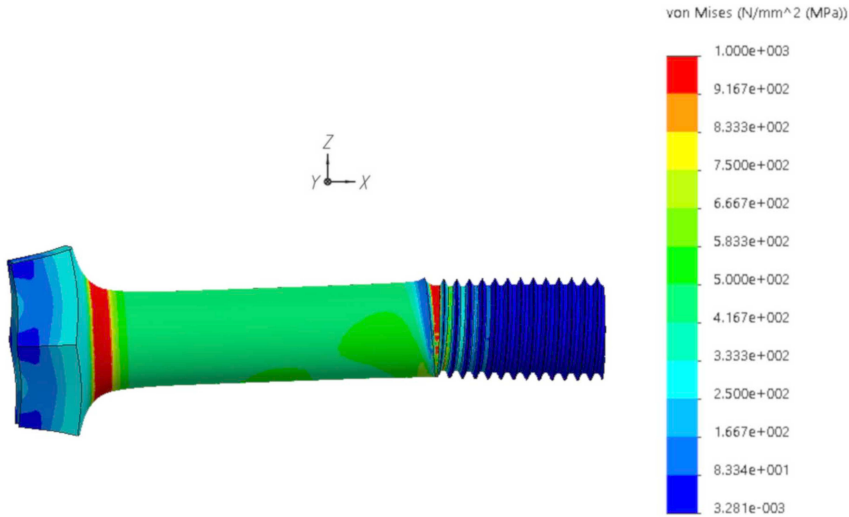


FIG. 6. Resultant displacements and scaled deformations in a high-strength bolt under prestressing.

Through the numerical analysis of the metric M24 10.9 grade high-strength bolt, according to the manufacturer [23] the maximum value of applied preload force, i.e. 225 552 N, has been shown that at the beginning of the thread (the plane connecting the bolt shank and thread), plastic MHS is obtained. The same situation occurs at the connection of the bolt head and shank. Due to the relatively high magnificent factor used in Fig. 5, one may notice that bolt failure would start at the bolt shaft – location of the thread commencement. On the threaded part of the bolt, the total cross-section area is lower than in other parts of the bolts. Hence, bolt failure would start at the threaded part due to the introduced preload force. Depending on the preload force value, nut location and number of threads in the nut as described in [3], two different failure modes can be observed – thread stripping or bolt fracture.

The bolt elongation along the X-axis which corresponds to the bolt longitudinal axis has been read out as  $-0.21$  mm. It should be noted that in practice the bolt elongation would be lower than the presented value – the washer located under the nut and the bolt head would be slightly pressed into the metal plate

and would deform slightly due to the bored hole being a larger size than the diameter of the bolt shaft.

#### 4. CONCLUSION

In this paper the static behaviour of a flange connection between two cylindrical tubes with high-strength bolts under preload and torsion moment forces as well as an authentically mapped single high-strength bolt under an applied preload have been discussed. Through the numerical analysis, deformations and stress distribution in both models have been presented. It has been shown that a numerical analysis may help to understand the process of stress arising in the considered parts of the structure; failure modes may also be determined. It is worth noting that a numerical analysis allows us to examine any object/phenomena in a very thorough way, which usually may be hard to observe through experimental studies. Despite that, experimental studies give more satisfactory results and show the actual behaviour of the examined object, whereas in a numerical analysis it is usually hard to define proper boundary conditions, which may cause incorrect results.

#### REFERENCES

1. The history of the bolt, <https://www.nord-lock.com/pl-pl/insights/knowledge/2017/the-history-of-the-bolt/> (22.02.2019).
2. HU Y., SHEN L., NIE S., YANG B., SHA W., *FE simulation and experimental tests of high-strength structural bolts under tension*, Journal of Constructional Steel Research, **126**: 174–186, 2016, doi: 10.1016/j.jcsr.2016.07.021.
3. GRIMSMO E.L., AALBERG A., LANGSETH M., CLAUSEN A.H., *Failure modes of bolt and nut assemblies under tensile loading*, Journal of Constructional Steel Research, **126**: 15–25, 2016, doi: 10.1016/j.jcsr.2016.06.023.
4. BLACHOWSKI B., GUTKOWSKI W., *Effect of damaged circular flange-bolted connections on behaviour of tall towers, modelled by multilevel substructuring*, Engineering Structures, **111**: 93–103, 2016.
5. PEIXOTO R.M., SEIF M.S., VIEIRA L.C.M., *Double-shear tests of high-strength structural bolts at elevated temperatures*, Fire Safety Journal, **94**: 8–21, 2017, doi: 10.1016/j.firesaf.2017.09.003.
6. LIU H., LIU D., CHEN Z., YU Y., *Post-fire residual slip resistance and shear capacity of high-strength bolted connection*, Journal of Constructional Steel Research, **138**: 65–71, 2017, doi: 10.1016/j.jcsr.2017.06.026.
7. GUO Z., LU N., ZHU F., GAO R., *Effect of preloading in high-strength bolts on bolted-connections exposed to fire*, Fire Safety Journal, **90**: 112–122, 2017, doi: 10.1016/j.firesaf.2017.04.030.

8. KODUR V., YAHYAI M., REZAEIAN A., ESLAMI M., POORMOHAMADI A., *Residual mechanical properties of high strength steel bolts subjected to heating-cooling cycle*, Journal of Constructional Steel Research, **131**: 122–131, 2017, doi: 10.1016/j.jcsr.2017.01.007.
9. KRISHNAMURTHY N., *A fresh look at bolted end-plate behavior and design*, Engineering Journal, **15**(2): 39–49, 1978.
10. MASHALY E., EL-HEWEITY M., ABOU-ELFATH H., OSMAN M., *Behavior of four-bolt extended end-plate connection subjected to lateral loading*, Alexandria Engineering Journal, **50**(1): 79–90, 2011, doi: 10.1016/j.aej.2011.01.011.
11. SELEJDAK J., KULIŃSKI K., MAJOR M., *Static analysis of a simple end-plate connection with high tensile bolts at different tightening torque using FEM software*, Proceedings of International Conference METAL 2017, (8p.) [in print].
12. SZAFRAN J., JUSZCZYK K., KAMIŃSKI M., *Experiment-based reliability analysis of structural joints in a steel lattice tower*, Journal of Constructional Steel Research, **154**: 278–292, 2019.
13. GRZEJDA R., *Modelling nonlinear preloaded multi-bolted systems on the operational state*, Engineering Transactions, **64**(4): 525–531, 2016.
14. FARMANI M.A., GHASSEMIEH M., *Shape memory alloy-based moment connections with superior self-centering properties*, Smart Materials and Structures, **25**(7): 075028, 2016, doi: 10.1088/0964-1726/25/7/075028.
15. MORADI S., ALAM M.S., *Feasibility study of utilizing superelastic shape memory alloy plates in steel beam-column connections for improved seismic performance*, Journal of Intelligent Material Systems and Structures, **26**(4): 463–475, 2015, doi: 10.1177/1045389X14529032.
16. FANG C., YAM M.C., MA H., CHUNG K.F., *Tests on superelastic Ni-Ti SMA bars under cyclic tension and direct-shear: towards practical recentring connections*, Materials and Structures, **48**(4): 1013–1030, 2015.
17. KREJSA M., BROZOVSKY J., MIKOLASEK D., KOUBOVA L., PARENICA P., MATERNA A., *Numerical modeling of fillet and butt welds in steel structural elements with verification using experiment*, Procedia Engineering, **190**: 318–325, 2017, doi: 10.1016/j.proeng.2017.05.344.
18. KORMANÍKOVÁ E., KOTRASOVÁ K., *Analysis and optimization of laminated circular cylindrical shell*, WSEAS Transactions on Applied and Theoretical Mechanics, 12, pp. 163–172, 2017, <http://www.wseas.org/multimedia/journals/mechanics/2017/a405911-057.pdf>.
19. MAJOR M., KULIŃSKI K., MAJOR I., *Dynamic analysis of an impact load applied to the composite wall structure*, MATEC Web of Conferences, **107**, 6 pages, 2017, doi: 10.1051/mateconf/201710700055.
20. KOZŁOWSKI A. [Ed.], *Steel structures. Numerical examples in accordance with PN-EN 1993-1-1. Part One. Chosen elements and connections* [in Polish: *Konstrukcje stalowe. Przykłady obliczeń wg PN-EN 1993-1-1. Część pierwsza. Wybrane elementy i połączenia*], Publishing House Rzeszow University of Technology, Rzeszów 2009.
21. BIEGUS A., *Designing of steel structures in accordance with Eurocode 3 – Part four: bolt connections* [in Polish: *Projektowanie konstrukcji stalowych według Eurokodu 3 – Część czwarta: Połączenia śrubowe*], Wrocław University of Technology Publishing House, Wrocław 2010.

22. *Supplementary information: Initial selection of a butt joint* [in Polish: Informacje uzupełniające: Wstępny dobór połączenia doczołowego prostego]. SN013a-PL-EU, <https://www.piks.com.pl/wp-content/uploads/2015/05/SN013a-PL-EU.pdf>
23. *Recommended maximum bolt loads and torque values* (Metric Coarse Threads), <https://alfadoctor.files.wordpress.com/2013/06/torque-chart.jpg> (accessed: November 30, 2018).

*Received December 26, 2018; accepted version February 14, 2019.*

---

*Published on Creative Common licence CC BY-SA 4.0*

